ELSEVIER

Contents lists available at ScienceDirect

Composites Part B

journal homepage: www.elsevier.com/locate/compositesb



Evaluation of fiber content in GFRP bars using digital image processing

Carlos N. Morales a, Guillermo Claure d, Jorge Álvarez b, Antonio Nanni a

- a Department of Civil Architectural and Environmental Engineering, University of Miami, Coral Gables, FL, 33146, USA
- b College of Engineering Johnson & Johnson 3D Printing Center of Excellence, University of Miami, Coral Gables, FL, 33146, USA

ARTICLE INFO

Keywords:

- A. Glass fibers
- A. Polymer-matrix composite (PMCs)
- B. Microstructure
- D. Electron microscopy

ABSTRACT

The tensile strength and elastic modulus of a fiber reinforced polymer (FRP) bar are directly related to the percentage of fibers measured by weight or volume. Recognizing the increasing number of different commercially available FRP bars, the implementation of precise methods for quantification of constituent fractions is of high importance to determine physico-mechanical properties. In this study, the fiber and resin matrix contents of four commercially available glass FRP (GFRP) bars were evaluated by implementing micrograph analysis of representative cross-sectioned specimens and compared to a conventional resin matrix separation method. The micrograph analysis was performed through digital image processing (DIP) of scanning electron microscope (SEM) images, while the conventional method was achieved by applying the standardized burn-off resin technique (ASTM D2584-18). The fiber volume fractions obtained from the DIP method were converted to weight fraction through constituent relationship equations. Comparable weight fraction values were obtained from both methods. However, the DIP method has the capability to provide additional microstructural information.

1. Introduction

Fiber reinforced polymer (FRP) bars, as internal reinforcement of concrete structures, have been shown to be a viable alternative to conventional steel reinforcement in highly corrosive environments [1]. The increasing demand and lack of strict standardization of this type of internal reinforcement has led to numerous FRP composite bars with different physical and mechanical properties [2]. These properties depend mainly on several factors, such as type of constituents, proportion of fibers to resin matrix, method of manufacture, and fiber orientations confined by the polymer matrix [3]. In FRP bars, since the matrix has significantly lower strength and stiffness than the fibers, the mechanical properties in the longitudinal direction largely depend on the fiber volume ratio, which is defined as the percentage of fiber volume with respect to the total volume of the composite [4].

The polymer matrix in FRP composites usually consist of a base resin binder, hardeners, fillers and additives [5,6]. While selection of an appropriate resin is critical for the pultrusion of quality products, the importance of additives and fillers which are combined with the neat resin to formulate the final matrix mix is of critical importance. Here is when different pultruders use their experience and knowledge in tweaking the production process. Functional fillers have gained acceptance as components of thermosetting pultrusion compounds. Not only

do they alter and contribute to the performance properties of the resin system but in some cases they also reduce production cost [5–7].

Some of the most commonly used inorganic fillers in pultruded composites are aluminum silicate, calcium carbonate and alumina trihydrate with typical density between 2400 and 2700 kg/m³ [8]. The amount of fillers in standard FRP bars usually vary between 15 and 20% by weight of the neat resin. As an example, for commercially available No. 3 (9.5 mm) GFRP bars, a manufacturer reports an average filler weight percentage of 3.97% for a given lot.

Determination of fiber content can be achieved by measuring the weight or volume of the composite constituents. When the basis of calculating the constituent contents is in terms of weights, it is expressed as "weight fraction" (wt%) and, when it is obtained by volume measurements, it is referred to as "volume fraction" (vol%). The three main methods to quantify the weight or volume fraction in a composite are resin burn-off (ignition loss), chemical digestion and micrographs analysis [6,9,10].

The first two are standardized methods (ASTM D2584-18 [11] and ASTM D3171-15 [12]) and are achieved by separating the fibers from the matrix and calculating the fiber content as a ratio of the original composite sample by weight. Of the two, the burn-off (BO) method cannot be used with fibers such as carbon or aramid as they would incinerate when exposed to high temperatures in the furnace.

E-mail addresses: cnm32@miami.edu (C.N. Morales), g.claure@umiami.edu (G. Claure), jalvarez@its.jnj.com (J. Álvarez), nanni@miami.edu (A. Nanni).

^{*} Corresponding author.

Irrespective of the fiber type, ASTM D2584-18 [11] is not ideal for assessing the fiber content in FRP bars intended for concrete reinforcement. In fact, these bars must have surface deformations (for example in the form of sand coatings, fiber wraps) that are necessary for the development of bond between bar and concrete. Additionally, inorganic fillers are sometimes present in the matrix that do not burn-off, prompting researchers to apply an alternative acid washout procedure to remove remnant fillers from the fibers [13,14].

The third method is accomplished by quantifying the fiber area fraction through magnified digital image processing (DIP) of a cross-sectional region of the composite, which can be obtained either by optical microscopy (OM) or scanning electron microscopy (SEM). This method assumes that the same cross-sectional profile extends across the length of the bar; therefore, in this study, the area fraction and volume fraction are considered to be the same. Even though the DIP is not a standardized method and has been used to a lesser extent, it has demonstrated to be an accurate and powerful tool to quantify composite microstructures [15,16]. Since the DIP method is a non-destructive assessment, FRP specimens can further be used for other types of material characterization, such as elemental composition through energy dispersive X-ray spectroscopy, identification of microstructural patterns and imperfections, distribution of constituents, and integrity of the fiber-resin interface.

The purpose of the present study is to evaluate the fiber and resin matrix content of FRP bars using the DIP method when compared to the standardized method of BO technique. The DIP technique could be an alternative to conventional destructive methods. Micrographs of the cross-sectional area of the composite were obtained using SEM. For reasons of economy, glass fibers are the most widely used for FRP bars as non-prestressed concrete reinforcement [2]. Thus, only commercially available glass FRP (GFRP) bars with the same nominal diameter were assessed as part of this research.

2. Experimental investigation

2.1. GFRP bar samples

In this study, four different types of pultruded GFRP bars, denoted as Type-A, -B, -C, and -D, were evaluated. The selected GFRP bars were produced by different pultruders; therefore, all of them exhibit different constituent compositions, properties, and surface enhancements. The surface treatment for each of the GFRP bars goes as follow: Type-A bars had a double helically-fiber-wrapped surface, Type-B bars had a four fiber-strand spiral winding surface, Type-C bars were made with spiral-ribbed deformed surface, and Type-D bars had a helically grooved surface. The surface treatment and, measured diameter and area (by immersion method), for each type of the GFRP bar assessed in this study are shown in Table 1.

For comparison purposes, all the GFRP bars evaluated in this study had the same nominal diameter of 9.5 mm and were not sand-coated.

Table 1Surface treatment and measured physical properties of GFRP bars.

Bar type	Surface treatme	ent	Diameter (mm)	Area (mm²)
A	Double helically- fiber- wrapped		9.56	71.8
В	Four fiber- strand spiral		9.16	65.9
С	Spiral-ribbed deformed	get in income	10.03	79.0
D	Helically grooved	13/11/11/11	9.81	75.5

Type-A, -B, and -D bars were made with ECR-glass fibers ($\rho_{f(ECR)}=2600~kg/m^3$), while Type-C bars with E-glass fibers ($\rho_{f(E)}=2500~kg/m^3$). In addition, all GFRP bars were made with vinyl ester ($\rho_r=1220~kg/m^3$) as the base resin in the matrix.

Since fillers represent a significant percentage of the matrix, for the purpose of this study, 17.5% by weight of the neat resin of aluminum silicate (kaolin) fillers with a typical density of 2580 kg/m³ was used to adjust the matrix densities. Also, due to the pigment added to the resin during manufacturing, 8% by weight of the matrix was added to the density of the GFRP bar Type-B. Taking these adjustments into account, the matrix densities (ρ_m) resulted in 1324 kg/m³ for GFRP bars Type-A, –C, and -D, and 1364 kg/m³ for GFRP bar Type-B.

3. Specimen preparation

3.1. Constituent content by weight

The fiber and resin content by weight for all the different GFRP bars type assessed this study were determined according to ASTM D2584-18 [11]. The principle of this test is to measure the fiber/resin weight fraction by burning the organic resin matrix in a muffle furnace at 565 °C and calculating its proportion with respect to the original weight of the composite. Since this test method only measures organic resin that burns completely at the specified temperature, caution must be taken when interpreting the fiber and resin fraction by weight. In this study, corrections were made to account for the remnant inorganic fillers. For each type of GFRP bar, four samples 25.4-mm long were cut and conditioned, as per standard, prior testing.

3.2. SEM

Sample preparation for either OM or SEM analysis is crucial and requires a highly polished surface to obtain optimal images [17]. Prior to imaging, GFRP bar samples must be carefully cut, ground and polished. Three samples 12.7-mm long were cut from each type of GFRP bar using a water-cooled precision saw (IsoMet 1000) with a diamond blade (IsoMet 15LC). To obtain a consistent highly polished surface, a semi-automatic grinding/polishing machine (LaboForce 100) was used. In order to facilitate this process, for each type of GFRP bar, samples were embedded in a cold-mounting epoxy resin "puck" (EpoFix).

Grinding and polishing of the surface was performed using the MD-System by Struers with several levels of abrasiveness ranging from 500 grit size to 0.04 μm polishing cloth. Different parameters, such as force, time, and rotational speed and direction of the sample holder and the platen, along with various water-based diamond suspension, were selected depending on the disc grit size. Before imaging, the specimens were placed in an oven for 24-h at a temperature of 50 $^{\circ} C$ to remove any possible moisture from the sample that may been absorbed during the process. The cross-sectional shape of the GFRP bars used in this study are shown in Fig. 1.

4. SEM imaging - DIP method

4.1. SEM images

SEM images were captured using a Zeiss EVO 60 SEM at the accelerating voltage of 20 kV. As it was important to distinguish between the different constituents (fiber, resin matrix and voids), the images were obtained using the backscattered electron (BSE) signal. Also, since GFRP bars are a non-conductive material and the samples were not sputter-coated with a conducting metal, the variable pressure (VP) mode was used. Considering that it is essential to obtain high-resolution SEM images, in this particular study, it was found that magnification level of $100 \times \text{produces}$ the largest field of view without sacrificing image quality. For each of the three GFRP bar samples in each epoxy puck,

Fig. 1. Cross-sectional area of GFRP bars Type-A, -B, -C, and -D (from left to right) encased in epoxy resin pucks.

three images were captured at 100 \times and stored with a resolution of 2048 \times 1536 pixels.

To be unbiased in the area where the images were taken, a procedure based on specific locations was established. The concept of the specified locations is to analyze representative area of the edge, center, and in between of the GFRP bar. In each of the embedded specimens, a GFRP bar was selected randomly and designated the number "1", the number "2" was given to the subsequent specimen located next to it clockwise and the number "3" was assigned to the remaining specimen. For the image locations, the designation goes as follow: the letter "X" for the top edge region, "Y" for halfway between the center and the right edge, and "Z" for the center. The images notation was based on the GFRP bar type (Type-A, -B, -C or -D), number of the sample (1, 2 or 3) and the location were the image was taken (region X, Y, or Z). The location for each image acquired, using the GFRP bar Type-A as an example, is shown in Fig. 2.

4.2. SEM image analysis

The backscatter electron images obtained from SEM were analyzed using *ImageJ*, a public domain open source image processing software.

The analysis consists in quantifying the percentage of fiber, resin matrix, and voids volume in each image using the threshold function. First, the original images had to be converted into 8-bit binary images (grayscale); this will change the interpretation of the images to integers in the range of 0-255. In the black and white spectrum, this will display the fibers as white, while the matrix resin will be displayed as grey and the voids as black area. Then, after the images were converted, the threshold function was used to show only specific ranges of intensity and to obtain the corresponding percentage based on the entire analyzed area. The lower range will only reveal the voids (darkest intensity), the mid-range will only show the matrix resin (grey intensity), while the upper range will only display the fibers (whitest intensity). To avoid overlaps and to quantify the entire spectrum (0–255), three unique display ranges of the threshold spectrum determined by the researcher were used for each of the analyzed images. Fig. 3 shows an example of the discussed DIP method for image A1Y, along with each corresponding histogram. The shaded area in Fig. 3b, c and d depict the range in the spectrum that is being revealed.

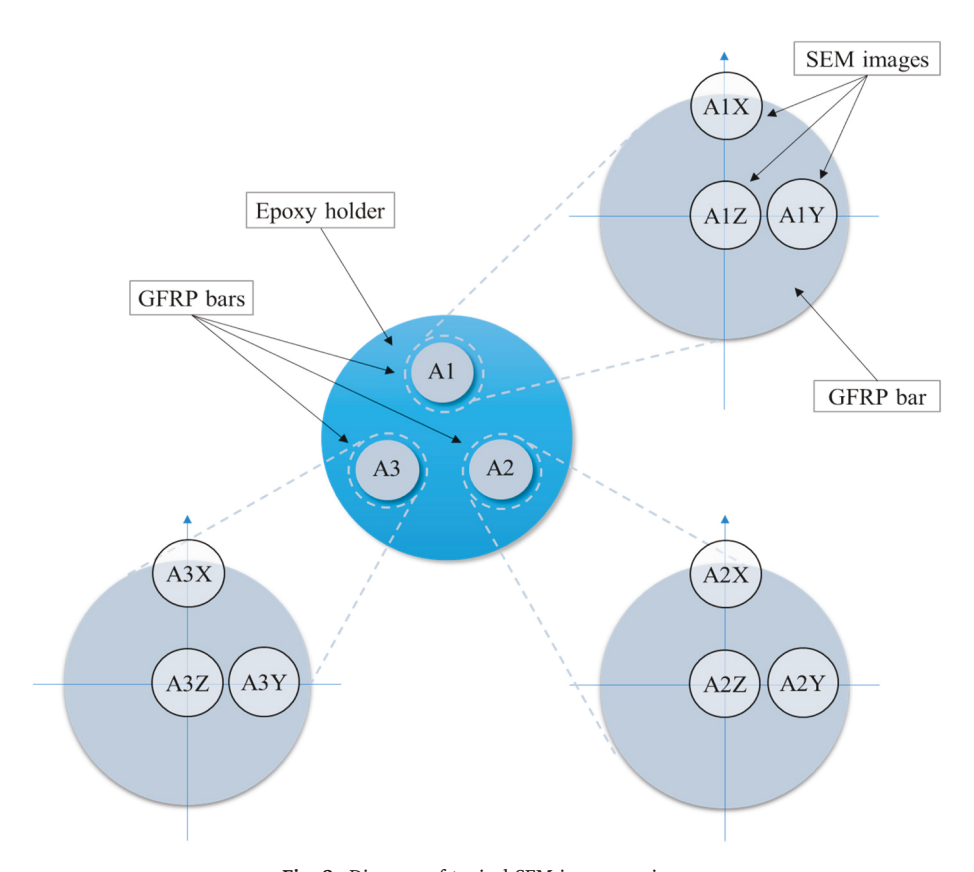


Fig. 2. Diagram of typical SEM images regions.

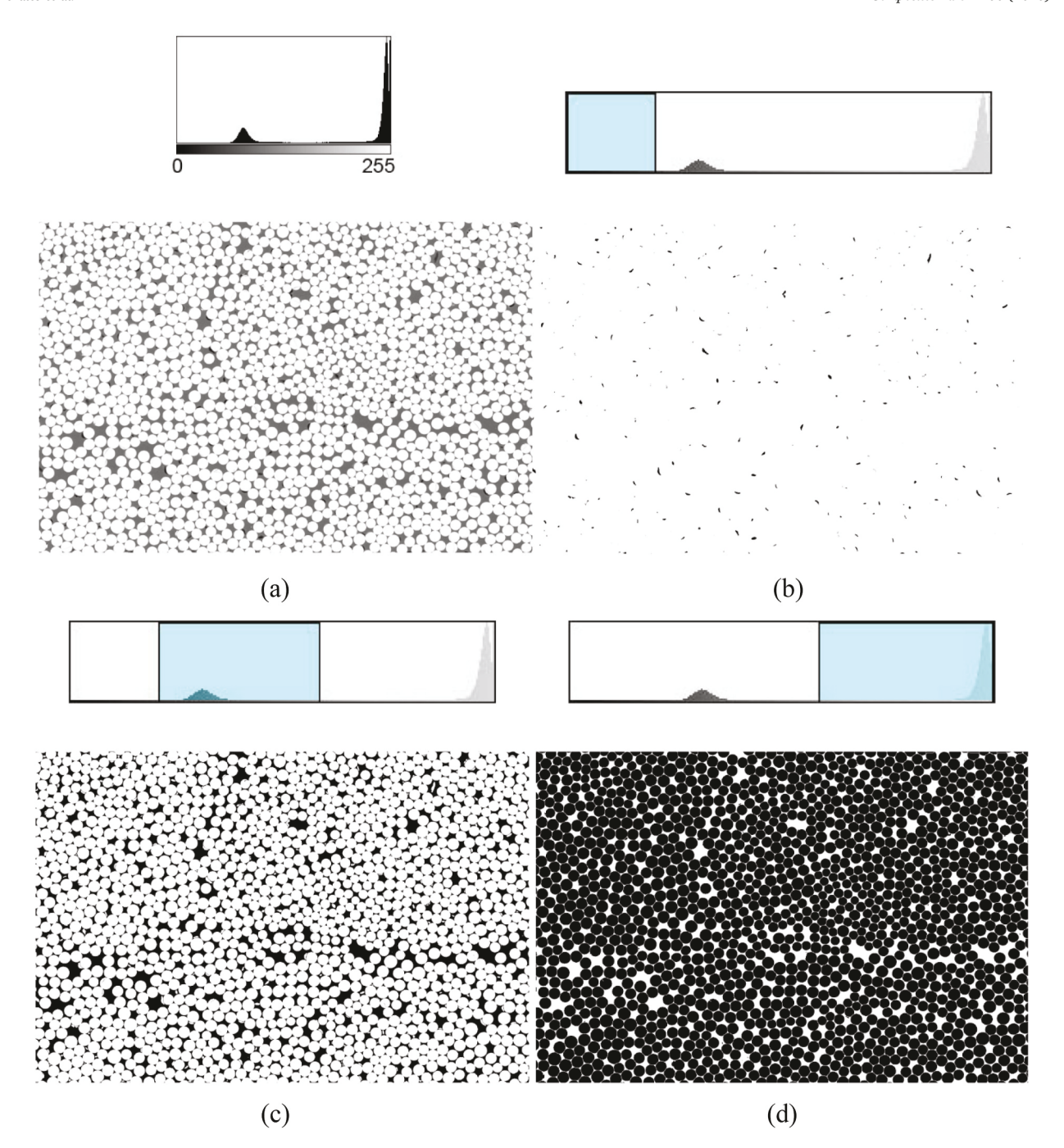


Fig. 3. Typical digital image processing method.

- (a) Original SEM image and histogram
- (b) Voids, i.e., low range threshold
- (c) Resin matrix, i.e., mid-range threshold
- (d) Glass fibers, i.e., upper range threshold.

4.3. Calculation

The weight fractions of the constituents of each type of GFRP bar, using the DIP method, were calculated as follows. For any number of constituents, in a given composite material, the sum of the constituent weight fractions must equal 1 [10,18]. For the GFRP bars evaluated in this study, the components were fiber and matrix material, which leads us to the following equation,

$$\omega_f + \omega_m = 1 \tag{1}$$

where ω_f , and ω_m are the weight fraction of the fiber and matrix, respectively. This equation assumes that the weight of the voids is negligible. The same analogy can be made for volume fraction:

$$v_f + v_m + v_v = 1 \tag{2}$$

where v_f , v_m and v_v , are the volume fraction of the fiber, matrix, and voids, respectively. The relationship between weight and volume fraction, for both fiber and resin, may be expressed as:

$$\omega_f = \frac{\rho_f}{\rho_c} v_f \tag{3}$$

and

$$\omega_m = \frac{\rho_m}{\rho_c} v_m \tag{4}$$

where ρ_f , ρ_m and ρ_c are the densities of fiber, matrix, and composite, respectively. Also, the density of a composites can be estimated through volume fractions and densities of the constituent materials [6,10,18], which leads us to the following expression ("rule of mixtures"):

$$\rho_c = \rho_f v_f + \rho_m v_m \tag{5}$$

Having all the parameters, ρ_f , ρ_m , ρ_c , ν_f , and ν_m , Eq. (3) and Eq. (4) were used to calculate the corresponding weight fraction of the fibers and resin matrix.

5. Experimental results and discussion

The average constituent volume percentages by region for each type of GFRP bars acquired by the DIP method are shown in Table 2. Considering the four types of GFRP bars, the mean fiber volume ranges from 55.45 to 72.64%, which is within the typical values for continuous fiber composite materials [6,19] and is above standard limit (CAN/CSA S807) for use in non-prestressed internal FRP reinforcement for concrete structures [14]. The standard deviation values reveal that in regions closer to the edge, the amount of fibers differs noticeably. For this reason, the fiber volume fraction in region X (edge) for GFRP bar Type-A, B and C was the smallest among the three regions, this can be attributed to the outer bar resin coating, while for GFRP bar Type-D was slightly higher indicating a more equal distribution of fibers along the edge and a smaller outer resin layer.

The average void content by region, among the four types of GFRP bars, varies from 0.02 to 0.92%. This broad range can be attributed to the irregular presence of voids within the cross-section. For instance, Fig. 4 (image B1Z) shows a considerable amount of manufacturing defects (voids) at a specific location. This is considered a "location-bias error" [20] and explains the high standard deviation of void content for GFRP bar Type-B. Despite the broad range, all GFRP bars had less than 1% of void content, which is ideal for the use of FRP bars as specified in CAN/CSA S807 [14].

Using Eq. (3) and Eq. (4), the average constituent volume fractions from region X, Y, and Z for each GFRP bar type obtained from the DIP method were converted to weight fraction. The equation to determine the composite densities, using the corresponding average constituent volume fraction obtained from the DIP method, is given in Eq. (5). In the BO method, the remnant inorganic fillers will alter the weight fraction values; therefore, to account for this, the established percentage (17.5% by weight of the neat resin) regarding the fillers was subtracted from the weight of fibers. The average fiber and resin matrix fraction by weight obtained from both methods, BO and DIP, as well as the difference between these two methods, are shown in Table 3 and are plotted in Fig. 5.

The highest difference between the fiber weight fraction obtain from BO and DIP was 3.27% points for GFRP bar Type-B, while the smallest was 0.83% points for GFRP bar Type-A. These differences can be attributed to the use of typical constituent properties instead of the precise values used by the each pultruders in the fabrication of the GFRP bars. This issue highlights the importance of the availability of product-specific information related to each lot supplied by the manufacturer. Also, since the fiber and resin weight fraction values obtained by the BO method are calculated as the ratio of remaining fibers with respect to the original weight of the composite, voids are neglected in this method. Considering the four GFRP bars tested in this study, the average fiber and resin weight fraction values agree within 1.69% between the two methods.

To date, only a handful of studies have been published on the evaluation of fiber content in composites using image analysis compared to conventional methods. Viens [21] investigated the fiber volume percentage of graphite/epoxy specimens by analyzing optical images (threshold technique) and implementing the standard acid digestion technique. He concluded that the results were within a 5% agreement between the two methods. Waterbury and Drzal [22] conducted a study on the fiber volume fraction of unidirectional graphite composite panels evaluated by optical image analysis (area method) and the chemical matrix digestion approach. They found that the results agree within better than 2.5% between the two methods. In another study, carried out by Cilley et al. [23], graphite/epoxy laminates were evaluated through different methods including acid digestion test and various quantitative microscopy techniques. The results indicated that the values between the acid digestion method and the areal analysis of micrographs agree within 2.16%.

It should be noted that the presented studies were conducted more than 30 years ago using optical imaging techniques that at this time would be considered obsolete. Thus, sharpness and resolution of images, that is of great importance in image processing, may have influenced the outcomes. While this may be true, the operational ease and readily available of more powerful equipment nowadays facilitate digital image acquisition and processing. Although SEM is the norm for performing microstructural characterization of FRP bars [24], optical microscopes with sufficient capability to capture high-resolution images, such as confocal laser scanning microscope, have been used [15].

In this study, taking into account that the analyzed micrographs had an area of 1137.8 $\mu m \times 763.9 ~\mu m$ (cropped data zone parameters), the average evaluated area at 100 \times among all the GFRP bars (9 images per GFRP bar type) was 11% with respect to the total cross-sectional area of the composite. It can be interpreted that the more images that are captured and analyzed, the more accurate results will be obtained, but the purpose of this study, for practical reasons, was to evaluate representative values with reasonable quantities of images.

Table 2Measured SEM DIP constituent volume percentages.

		Average	SD	Average	SD	Average	SD
Bar type	SEM image region	Fiber, v_f (%)		Matrix, v_m (%)		Voids, ν _ν (%)	
Α	X	68.02	7.44	31.09	7.21	0.89	0.27
	Y	72.63	1.17	26.88	1.21	0.49	0.09
	Z	72.64	1.29	26.73	1.38	0.63	0.10
В	X	60.34	5.07	39.24	5.35	0.42	0.30
	Y	62.85	2.09	37.05	2.10	0.10	0.05
	Z	62.88	3.35	36.20	1.95	0.92	1.42
C	X	55.45	5.28	44.28	5.29	0.27	0.23
	Y	61.31	0.38	38.67	0.37	0.02	0.01
	Z	59.03	0.73	40.95	0.73	0.02	0.01
D	X	67.60	3.94	32.28	3.95	0.12	0.01
	Y	66.79	0.78	33.16	0.79	0.05	0.01
	Z	66.32	3.37	33.61	3.39	0.06	0.03

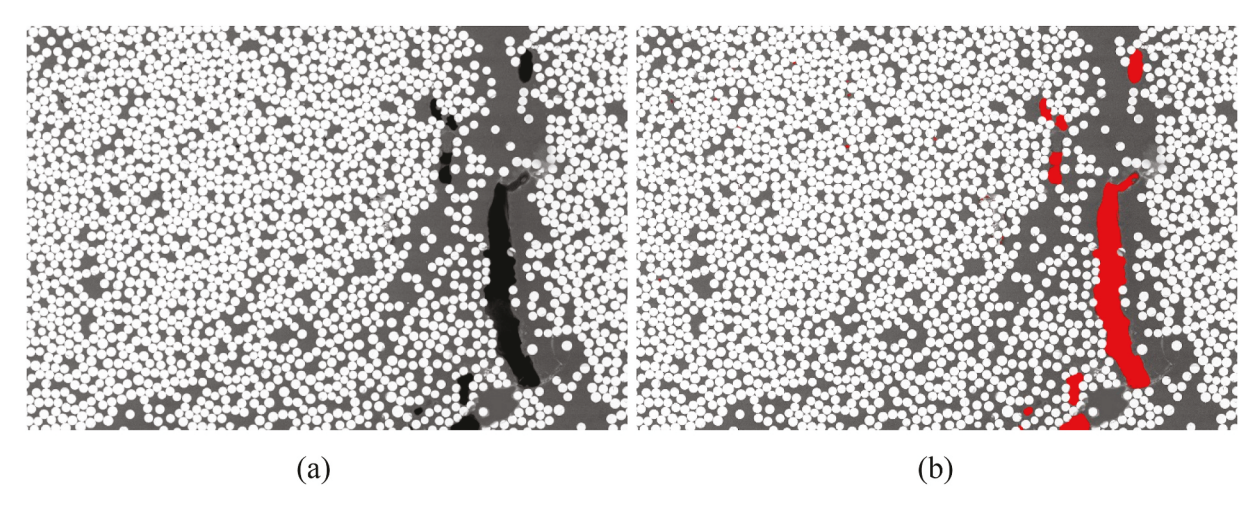


Fig. 4. High concentration of voids in the core of GFRP bar Type-B.

- (a) Original SEM image
- (b) Location of voids highlighted in red.. (For interpretation of the references to colour in this figure legend, the reader is referred to the Web version of this article.)

Table 3Fiber and resin weight fractions determined by BO and DIP methods.

Bar type	Fiber weight fraction, ω_f (%)				Percentage point difference ^a	
	ВО		DIP			
	Average	SD	Average	SD		
A	82.45	0.20	83.28	5.23	0.83	
В	72.44	0.17	75.71	4.21	3.27	
C	71.51	0.62	72.82	4.60	1.31	
D	78.64	0.28	79.98	3.20	1.34	
	Matrix weight fraction, ω_m (%)					
	ВО		DIP			
	Average	SD	Average	SD		
A	17.55	0.20	16.72	2.54	0.83	
В	27.56	0.17	24.29	2.16	3.27	
C	28.49	0.62	27.18	2.38	1.31	
D	21.36	0.28	20.02	1.64	1.34	
	Average				1.69	

^a Difference calculated as.|BO - DIP|

6. Summary and conclusions

Four different types of commercially available pultruded GFRP bars with a nominal diameter of 9.5 mm were evaluated. Burn-off and digital image processing methods were used to quantify the fiber and resin matrix weight fractions for all the GFRP bars assessed this study. For the BO method, specimens 25.4-mm long were tested, according to the standard. SEM images were performed at $100 \times \text{magnification}$ and the fiber and resin volume fractions were evaluated using the DIP thresholding technique. Then, the fiber and resin matrix weight fractions were calculated using established relationships. In accordance with the results obtained by the two methods, the following observations are made.

- The DIP method was successfully performed and provided direct quantifiable values of the volume fraction of each constituent.
- Unlike composite matrix separation methods, the DIP method has the capability to provide additional microstructural information such as fiber distribution, imperfections, and presence of voids.
- Even though the percentage of fiber and resin weight fraction in each of the GFRP bars turned out to be different, they were all above the

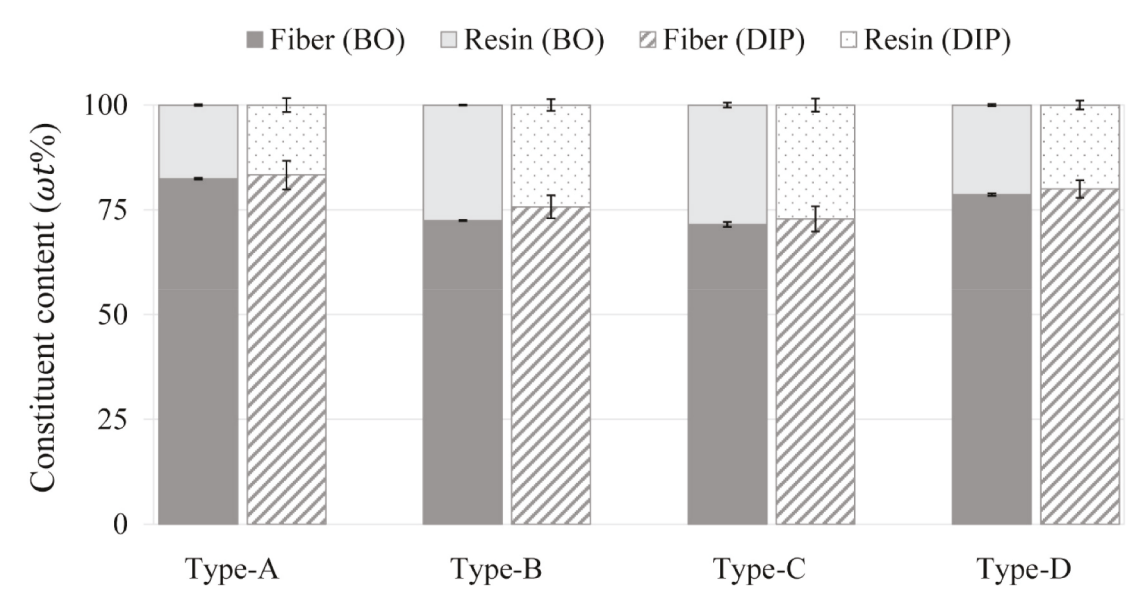


Fig. 5. GFRP bars constituent content, in percentage by weight, determined by BO and DIP methods. Error bars represent 95% confidence intervals.

limit of 70% by weight commonly specified in standards such as ASTM D7957-17 and CSA S807-10 [14,25].

- Comparable results were obtained from the two methods, which are
 in agreement with those reported in the literature. The differences
 can be credited to the use of assumed typical constituent properties
 and contents instead of the actual values used by the manufacturers.
- Analysis of 11% (9 images per GFRP type at 100 ×) of the total crosssectional area of the GFRP bar using the DIP method was sufficient to obtain representative results when compared to the BO method. However, the random nature of clustered voids and defects can lead to an under/over-assessment of their volume fractions.
- The weight fraction values obtained from the DIP method depend on the quantity and density of the individual constituents; in fact, perhaps the actual volume fraction of fibers, resin matrix, and voids obtained directly from the DIP method are more relevant and reliable to assess mechanical properties than the percentages of constituent content obtained by weight (BO method).

The conclusions reached in this study using the DIP method emphasize the relevance and practicality of obtaining direct quantification of fiber, resin matrix and voids volume as opposed to fiber and resin content by weight. Furthermore, the DIP method could be useful when additional microstructural evaluations are required.

CRediT authorship contribution statement

Carlos N. Morales: Conceptualization, Methodology, Validation, Formal analysis, Investigation, Writing - original draft, Visualization. Guillermo Claure: Conceptualization, Methodology, Writing - review & editing, Supervision. Jorge Álvarez: Methodology, Investigation, Resources. Antonio Nanni: Writing - review & editing, Supervision, Funding acquisition.

Declaration of competing interest

The authors declare that they have no known competing financial interests or personal relationships that could have appeared to influence the work reported in this paper.

Acknowledgements

The authors gratefully acknowledge the financial support from the Qatar National Research Fund by the grant # NPRP9-110-2-052 and the National Science Foundation (NSF) and its Industry/University Center for the Integration of Composites into Infrastructure (CICI) at the University of Miami under the grant # NSF-1916342.

References

Gooranorimi O, Nanni A. GFRP reinforcement in concrete after 15 Years of service.
 J Compos Construct 2017;21:04017024. https://doi.org/10.1061/(ASCE)CC.1943-5614.0000806.

- [2] Emparanza AR, Kampmann R, De Caso y Basalo F. State-of-the-practice of global manufacturing of FRP rebar and specifications. Am Concr Institute, ACI Spec Publ; 2017;2017-Octob. 717–30.
- [3] Hollaway LC. Key issues in the use of fibre reinforced polymer (FRP) composites in the rehabilitation and retrofitting of concrete structures. In: Serv. Life estim. Ext. Civ. Eng. Struct. Elsevier Ltd; 2010. p. 3–74.
- [4] ACI Committee 440. Guide for the design and construction of structural concrete reinforced with fiber-reinforced polymer (FRP) bars (ACI 440.1R-15). American Concrete Institute; 2015.
- [5] Bai J. Advanced fibre-reinforced polymer (FRP) composites for structural applications. Sawston: Cambridge: Woodhead Publishing Limited; 2013. https://doi.org/10.1533/9780857098641.
- [6] Zoghi M. The international handbook of FRP composites in civil engineering. Boca Raton, Florida: CRC Press/Taylor & Francis Group; 2014.
- [7] Nanni A, De Luca A, Jawaheri Zadeh H. Reinforced concrete with FRP bars: mechanics and design. Boca Raton, Florida: CRC Press/Taylor & Francis Group; 2014. https://doi.org/10.1201/b16669.
- [8] Bank LC. Composites for construction: structural desing with FRP materials. Hoboken, NJ, USA: John Wiley & Sons, Inc.; 2006. https://doi.org/10.1002/9780470121429
- [9] Carlsson LA, Adams DF, Pipes RB. Experimental characterization of advanced composite materials. fourth ed. Boca Raton: CRC Press; 2014. https://doi.org/ 10.1201/b16618.
- [10] Gibson RF. Principles of composite material mechanics. third ed. Boca Raton: CRC Press; 2011. https://doi.org/10.1201/b14889.
- [11] ASTM D2584. Standard test method for ignition loss of cured reinforced resin. West Conshohocken (PA): ASTM International; 2018.
- [12] ASTM D3171. Standard test methods for constituent content of composite materials. West Conshohocken (PA): ASTM International; 2015.
- [13] Benzecry V, Brown J, Al-Khafaji A, Haluza R, Koch R, Nagarajan M, et al. Durability of GFRP bars extracted from bridges with 15 to 20 Years of service life. 2019.
- [14] CAN/CSA S807-10. Specification for fibre-reinforced polymers. Ontario, Canada: Canadian Standards Association; 2010.
- [15] Conklin L. Tutorial for collecting and processing images of composite structures to determine the fiber volume fraction. Natl Inst Aerospace; NASA 2017.
- [16] Paciornik S, D'Almeida JRM. Measurement of void content and distribution in composite materials through digital microscopy. J Compos Mater 2009;43:101–12. https://doi.org/10.1177/0021998308098234.
- [17] Mukhopadhyay SM. In: Sample preparation for microscopic and spectroscopic characterization of solid surfaces and films. Sample prep. Tech. Anal. Chem. Hoboken, NJ, USA: John Wiley & Sons, Inc.; 2003. p. 377–411. https://doi.org/ 10.1002/0471457817.ch9.
- [18] Kaw AK. Mechanics of composite materials. second ed. Boca Raton: CRC Press; 2005. https://doi.org/10.1201/9781420058291.
- [19] Balaguru P, Nanni A, Giancaspro J. FRP composites for reinforced and prestressed concrete structures. New York & London: CRC Press/Taylor & Francis Group; 2009. https://doi.org/10.1201/9781482288537.
- [20] Mehdikhani M, Gorbatikh L, Verpoest I, Lomov SV. Voids in fiber-reinforced polymer composites: a review on their formation, characteristics, and effects on mechanical performance. J Compos Mater 2019;53:1579–669. https://doi.org/ 10.1177/0021998318772152.
- [21] Viens MJ. Determination of fiber volume using in graphite/epoxy materials computer image analysis. Natl Aeronaut Sp Adm 1990.
- [22] Waterbury MC, Drzal LT. Determination of fiber volume fractions by optical numeric volume fraction analysis. J Reinforc Plast Compos 1989;8:627–36. https://doi.org/10.1177/073168448900800605.
- [23] Cilley E, Roylance D, Schneider N. Methods of fiber and void measurement in graphite/epoxy composites. Compos Mater Test Des (Third Conf 2009. https://doi. org/10.1520/stp35492s. 237-237-13.
- [24] El-Hassan H, El Maaddawy T. Microstructure characteristics of GFRP reinforcing bars in harsh environment. Ann Mater Sci Eng 2019;2019:1–19. https://doi.org/ 10.1155/2019/8053843.
- [25] ASTM D7957. Standard specification for solid round glass fiber reinforced polymer bars for concrete reinforcement. 2017. West Conshohocken (PA).